Dual-time-point 18F-FDG PET imaging for diagnosis of disease type and disease activity in patients with idiopathic interstitial pneumonia

TITLE PAGE

Full article title: Dual-time-point ^{18}F-FDG PET Imaging for Diagnosis of Disease Type and Disease Activity in Patients with Idiopathic Interstitial Pneumonia

Full first and last name: Yukihiro Umeda, MD[1], Yoshiki Demura MD, PhD[1] Takeshi Ishizaki MD PhD[1], Shingo Ameshima MD PhD[1], Isamu Miyamori MD PhD[2], Yuji Saito MD PhD[3], Tatsuro Tsuchida MD PhD[4], Yasuhisa Fujibayashi PhD[5], Hidehiko Okazawa MD PhD[5]

Institutional affiliation:

[1]Department of Respiratory Medicine, University of Fukui

23-3 Matsuokashimoaizuki, Eiheiji-cho, Yoshida-gun Fukui 910-1193 Japan

[2]Third Department of Internal Medicine, University of Fukui

23-3 Matsuokashimoaizuki, Eiheiji-cho, Yoshida-gun Fukui 910-1193 Japan

[3]Division of Respirology & Allergology, Department of Internal Medicine, School of Medicine, Fujita Health University

1-98 Dengakugakubo, Kutsukake-cho, Toyoake, Aichi 470-1192 Japan

[4]Department of Radiology, University of Fukui

23-3 Matsuokashimoaizuki, Eiheiji-cho, Yoshida-gun Fukui 910-1193 Japan

[5]Biomedical Imaging Research Center, University of Fukui

23-3 Matsuokashimoaizuki, Eiheiji-cho, Yoshida-gun Fukui 910-1193 Japan

Corresponding author: Yoshiki Demura, Department of Respiratory Medicine, University of Fukui, 23-3 Matsuokashimoaizuki, Eiheiji-cho, Yoshida-gun Fukui 910-1193 Japan

[e-mail address] DEM2180@aol.com

[Telephone] +81-(0)776-61-3111 [Fax] +81-(0)776-61-8111

ABSTRACT

Purpose Individual clinical courses of idiopathic interstitial pneumonia (IIP) are variable and difficult to predict because the pathology and disease activity are contingent, and chest computed tomography (CT) provides little information about disease activity. In this study, we applied dual-time-point [^{18}F]-fluoro-2-deoxy-*D*-glucose (^{18}F-FDG) positron emission tomography (PET), commonly used for diagnosis of malignant tumors, to the differential diagnosis and prediction of disease progression in IIP patients.

Methods Fifty patients with IIP, including idiopathic pulmonary fibrosis (IPF, n=21), nonspecific interstitial pneumonia (NSIP, n=18), and cryptogenic organizing pneumonia (COP, n=11), underwent ^{18}F-FDG PET examinations at two time points: Scan 1 at 60 min (early imaging) and Scan 2 at 180 min (delayed imaging) after ^{18}F-FDG injection. The standardized uptake values (SUV) at the two points and the retention index (RI-SUV) calculated from them were evaluated and compared with chest CT findings, disease progression, and disease types. To evaluate short term disease progression, all patients were examined pulmonary function test every 3 months for 1 year after ^{18}F-FDG PET scanning.

Results The early SUV for COP (2.47±0.74) was significantly higher than that for IPF

(0.99±0.29, *P*=0.0002) or NSIP (1.22±0.44, *P*=0.0025). When an early SUV cut-off value of 1.5 and greater was used to distinguish COP from IPF and NSIP, the sensitivity, specificity, and accuracy were 90.9%, 94.3%, and 93.5%, respectively. The RI-SUV for IPF and NSIP lesions was significantly greater in patients with deteriorated pulmonary function after 1-year of follow-up (progressive group, 13.0±8.9%) than in cases without deterioration during the 1-year observation period (stable group, -16.8±5.9%, *P*<0.0001). However, the early SUV for all IIP types provided no additional information of disease progression. When an RI-SUV cut-off value of 0% and greater was used to distinguish progressive IIPs from stable IIPs, the sensitivity, specificity, and accuracy were 95.5%, 100%, and 97.8%, respectively.

Conclusion Early-SUV and RI-SUV obtained from dual-time point ^{18}F-FDG PET are useful parameter for the differential diagnosis and prediction of disease progression in patients with IIP.

Key Words: idiopathic interstitial pneumonia; dual-time point; ^{18}F-FDG PET; disease activity, differential diagnosis, retention index

INTRODUCTION

The idiopathic interstitial pneumonias (IIPs) are a heterogeneous group of disorders resulting from damage to the lung parenchyma due to varying patterns of inflammation and fibrosis. Idiopathic pulmonary fibrosis (IPF), nonspecific interstitial pneumonia (NSIP), and cryptogenic organizing pneumonia (COP) comprise the majority of IIP cases. Distinguishing different types of IIP is important because COP is known to show a better prognosis than IPF and NSIP [1].

Management of patients with IIP is challenging, as many factors are involved, including difficulties with diagnosis and determination of disease activity. However, along with greater understanding of the clinical course and pathophysiology of this group of disorders, a recent consensus statement provided a clearer framework for both diagnosis and management [1]. Classification of IIPs is based on histopathological patterns of the disease from surgical lung biopsy specimens, as well as clinical and computed tomography (CT) findings. However, predicting disease progression is less certain in IIP. Chest CT shows changes in lung density but can give no indication of disease activity. Although histopathological diagnosis is related to survival in IIP patients, individual clinical courses are highly variable and unpredictable. Furthermore, thoracic surgical procedures are stressful for IIP patients [2, 3] and hazardous to repeat,

therefore should be avoided unless absolutely necessary, while lung segment samples may not accurately represent the lung as a whole [4].

Other noninvasive, real-time measures of lung inflammation in IIP patients, which can predict the disease activity, are expected. External imaging using radiolabeled markers of inflammatory processes has great potential for providing a noninvasive and repeatable test for monitoring inflammatory cell behavior. [^{18}F]-2-fluoro-2-deoxy-*D*-glucose positron emission tomography (^{18}F-FDG PET) is an imaging modality that detects the increased uptake of glucose in areas of increased cell metabolism. This technique is most often applied for diagnosis of malignancy, although it has also been found useful for detection of benign diseases [5], such as bronchiolitis obliterans organizing pneumonia (BOOP) [6], IPF [7], and drug-induced pneumonitis [8].

Recently, dual-time point ^{18}F-FDG PET has been reported as useful for not only diagnosing malignancy but also for assessing the disease activity of benign inflammatory diseases, such as tuberculoma [9]. *In vitro* models of activated inflammatory cells, such as macrophages, lymphocytes, and neutrophils, have been reported to have significantly increased FDG uptake [10-12]. Activation of these inflammatory cells causes a sustained increase in FDG accumulation over time. Thus,

we hypothesized that it might be possible to use dual-time point ^{18}F-FDG PET imaging in patients with IIP to assess the degree of inflammation, and to provide predictive information of disease progression. In the present study, we evaluated the potential role of dual-time point ^{18}F-FDG PET for elucidation of disease progression and histopathologic diagnosis (disease type) in patients with IIP.

MATERIALS AND METHODS

Study Population

We enrolled 53 consecutive patients with IIP who were treated at the University of Fukui Hospital between January 2004 and December 2007. Three patients were subsequently excluded after being diagnosed with other diseases (1 case of malignant disease, 2 cases of collagen vascular disease). Patients with a defined connective tissue disease, left ventricular failure, occupational and/or environmental exposure that resulted in interstitial pneumonia, or history of ingestion of a drug or agent known to cause pulmonary fibrosis were excluded from the study. Thus, 50 patients (21 men, 29 women; age range, 21-84 years old; mean age ± SD, 66.2±11.6 years) were included in the present study. This study was approved by the Institutional Review Board of the hospital and written informed consent was obtained from all participating patients. All 50 patients had untreated IIP, and were comprised of 21 with IPF, 18 with NSIP, and 11 with COP (Table 1). None of the subjects had received steroids or immunosuppressants at the time of clinical sample collection. Degree of dyspnea was scored from 0 to 20, with a higher score indicating more severe dyspnea [13]. Pulmonary function tests [spirometry, measurement of lung volumes, and diffusing capacity of the lungs measured using carbon monoxide (D_{LCO})] were performed in all patients according to

the American Thoracic Society/European Respiratory Society (ATS/ERS) guidelines [14]. Arterial blood gas analysis was performed in all patients within a period of one week before ^{18}F-FDG PET scan. Fiberoptic bronchoscopy was performed in all patients within a period of two weeks after the ^{18}F-FDG PET scan. Thereafter, 32 patients underwent a surgical lung biopsy within four weeks of the ^{18}F-FDG PET scan.

Of the 21 patients with IPF, nine were diagnosed clinically, and pathologically confirmed as having a usual interstitial pneumonia (UIP) pattern on the basis of surgical lung biopsy results, and 12 were diagnosed as having clinical IPF according to the ATS clinical diagnostic criteria [15]. All 18 patients with idiopathic NSIP were diagnosed clinically, and pathologically confirmed fibrotic NSIP pattern on the basis of surgical lung biopsy results. All 11 patients with COP (i.e. idiopathic BOOP in pathology) were diagnosed clinically, and pathologically confirmed on the basis of surgical lung biopsy results (n=5), or a transbronchial lung biopsy (n=6). Pathological diagnoses were made according to ATS/ERS classification criteria [1]. These specimens were reviewed by at least two pathologists in the hospital's pathology department without prior knowledge of the ^{18}F-FDG PET results.

Measurement of Serum markers

We assessed serum levels of Krebs von den Lungen-6 (KL-6) and surfactant proteins-D (SP-D) in all patients within a period of two weeks before the ^{18}F-FDG PET scan. Serum KL-6 and SP-D were quantitatively determined using enzyme-linked immunosorbent assay [(KL-6: Sanko Junyaku; Tokyo, Japan), (SP-D: Yamasa; Chiba, Japan)]. Since no serum controls were available for this study, we used the normal range in healthy individuals provided by the manufacturer (KL-6: 94.9 to 458.2 U/mL, SP-D: 18.6 to 79.4 ng/mL).

Thoracic CT

Patients underwent CT scanning with a 16-detector row CT (Sensation 16; Siemens, Erlangen, Germany) system before ^{18}F-FDG PET scanning. Contiguous 5.0 mm thick sections were initially obtained at 5.0 mm intervals throughout the thorax, followed by non-contrast chest high-resolution (HR) CT, which was used to obtain 2.0 mm cross-sectional slices at 10 mm intervals throughout the thorax. All images were reconstructed using a bone algorithm and obtained at window settings suitable for viewing lung parenchyma.

HRCT findings for abnormal lesions were defined as follows; “honeycomb”, including honeycomb change, “consolidation”, including air-space consolidations, and

“ground grass opacities (GGO) and reticular density”, including diffuse GGO and reticular densities; HRCT findings with no abnormal shadows were defined as “normal”.

^{18}F-FDG PET

^{18}F-FDG PET imaging was performed using a whole-body scanner (ADVANCE; General Electric Medical Systems; Milwaukee, WI). All patients fasted overnight (for at least 12 hours) before radiotracer administration. None had insulin-dependent diabetes, and the serum glucose level was below 126 mg/dl in all patients immediately before the injection of ^{18}F-FDG. Approximately 185 MBq of ^{18}F-FDG (a dose commonly used for clinical ^{18}F-FDG PET scans in Japan) was intravenously administered. Emission scans of the thorax were obtained one hour later for 20 minutes (early scan), then three hours later for 20 minutes (delayed scan). A transmission scan was obtained for 10 minutes using a standard rod source of ^{68}Ge/^{68}Ga for attenuation correction before each emission scan at the same bed position as the emission scan. For each emission scan, the patient’s body was carefully positioned with laser beam guidance to prevent misregistration. Images were viewed as transaxial slices of the thorax with a slice thickness of 4.25 mm.

PET Image Interpretation

Semiquantitative analysis of ^{18}F-FDG uptake was based on region of interest (ROI) analysis, which produced mean standardized uptake values (SUV) [= (local radioactivity concentration) / (injected dose) / (body weight)]. After PET and CT images were coregistered using a specific software (Body Guide; Advance Biologic, Toronto, Canada), circular ROIs with a fixed size of 30 mm in diameter were drawn on the CT images in the anterior, lateral, and posterior sites of the bilateral lungs (Fig. 1) at three representative slice levels; the upper lung field, considered to be at the level of the aortic arch; the middle lung field, considered to be at the level of tracheal bifurcation; and the lower lung field, considered to be above the level of the diaphragm. The ROIs were placed by two experienced radiologists. For comparison of images acquired at 1 and 3 hours, the same ROIs were applied to both early and delayed PET images of the same CT level. The retention index (RI-SUV) was calculated from the SUV levels of one hour (early SUV) and three hours (delayed SUV) using the following equation:

RI-SUV (%) = (delayed SUV – early SUV) × 100/ early SUV.

For analysis of ^{18}F-FDG uptake in IIP lesions, SUV levels of each lesion, assessed by the ROI method, were classified according to CT findings. The early SUV and RI-SUV for lesions were averaged for ROIs of lesions that had an abnormal shadow (honeycomb,

consolidation, GGO and reticular density) on corresponding HRCT images. The early SUV and RI-SUV for normal lung fields were averaged among all ROIs without any abnormal shadow on corresponding HRCT images. The averaged early SUVs and RI-SUVs of the abnormal shadows, as well as normal lung, were compared between diseases.

Clinical Reevaluation

To evaluate short-term disease progression of IIP, we examined all patients at least every 3 months for 1 year after ^{18}F-FDG PET scanning to determine whether their condition with regard to the disease had improved or remained the same (stable IIP) or deteriorated (progressive IIP). Patients were not given any steroid or other immunosuppressant therapy. Progressive IIP was defined according to ATS criteria [14], and included patients who had evidence of deterioration within 12 months after ^{18}F-FDG PET scanning in regard to pulmonary function in two or more of the following categories: a 10% decrease in total lung capacity or vital capacity (or ≥200-mL change), a 15% decrease in single-breath D_{LCO} (or at least ≥3-ml/min/mmHg change), worsening (greater fall) of O_2 saturation (≥4 percentage point decrease in the measured saturation), or a rise in alveolar-arterial oxygen pressure difference ($AaDO_2$) at rest (≥4 mmHg

increase from the previous measurement). Patients who did not show deterioration over the 1-year observation period were defined as having stable IIP.

Statistical Analysis

All values express the mean ± SD. Differences in SUV and RI-SUV level and clinical data among multiple groups were determined with non-parametric Kruskal-Wallis test and Steel-Dwass test to assess between-group comparisons. For all analyses, *P* values less than 0.05 were considered to be statistically significant.

RESULTS

Subject and Clinical Characteristics

Patient characteristics are shown in Table 1. Of the 50 patients with IIP, 25 showed deterioration during the 1-year observation period (progressive IIP 50.0%). These 25 were comprised of 8 of the 21 patients with IPF (progressive IPF 38.1%), 9 of the 18 with NSIP (progressive NSIP 50.0%), and 8 of the 11 with COP (progressive COP 72.7%).

Table 2 outlines dyspnea score, serum markers, arterial blood gas analysis, and pulmonary function data of study participants. The KL-6 levels of patients with IPF and NSIP were higher than those of patients with COP, whereas there was no difference in SP-D. The resting arterial partial pressure of oxygen (PaO_2) of patients with IPF and NSIP was higher than that of patients with COP. There were no differences between disease types in dyspnea score, vital capacity (VC), and D_{LCO}.

HRCT findings

Table 2 also shows the findings of HRCT. About 90% of patients with IPF had a dominant honeycombing pattern with some degree of GGO or reticular density. For NSIP, all patients had GGO and reticular density as the dominant pattern and about half

of the patients had consolidation. Only three patients had honeycombing. About 90% of patients with COP had consolidation and/or GGO.

Period between ^{18}F-FDG PET scan and Initiation of Therapy

Of 25 patients with progressive IIP, 19 (three of eight progressive IPF, eight of nine progressive NSIP, and all eight progressive COP) were treated during 1-year follow-up. The median period between PET scan and initiation of therapy was 96 days (range, 90-150 days) for IPF patients, 49.5 days (range, 30-353 days) for NSIP, and 34.5 days (range, 20-40 days) for COP.

^{18}F-FDG PET in IIP

Figure 2A shows the distribution of early SUV levels for lung lesions in patients with IIPs. Table 3 shows the mean early SUV level in patients with IIP according to CT findings. The early SUV of lung lesions, defined as abnormal shadows on CT images, was significantly higher than that in normal lung areas (normal) in all three IIP groups. The early SUV of lung lesions in COP (2.47±0.74) was significantly higher than that in IPF (0.99±0.29, $P = 0.0002$, analyzed by the Steel-Dwass test) or NSIP (1.22±0.44, $P = 0.0025$). Receiver operating characteristic (ROC) curve analysis determined that the

most suitable cut-off value for early SUV at lung lesions was 1.5 to distinguish COP from the IPF and NSIP groups. When this threshold for early SUV was used to diagnose COP, sensitivity, specificity, and accuracy of ^{18}F-FDG PET were 90.9%, 94.3%, and 93.5%, respectively. In addition, when the analysis was limited to surgically confirmed cases, the early SUV of lung lesions in COP (2.66±0.82, n=5) was significantly higher than that in IPF (0.94±0.25, P = 0.0072, analyzed by the Steel-Dwass test, n=9) or NSIP (1.22±0.44, P = 0.0036, n=18). In surgically confirmed cases, when early SUV of 1.5 was used to diagnose COP, sensitivity, specificity, and accuracy of ^{18}F-FDG PET were 100%, 96.3%, and 96.9%, respectively.

Table 4 shows the comparison of early SUV in each lesion type according to chest HRCT findings. In patients with IPF, NSIP and COP, the early SUV level of honeycomb and consolidation on corresponding HRCT images was significantly higher than that of GGO and reticular density. However, there was no difference between honeycomb and consolidation in patients with IPF and NSIP.

Disease Progression and Dual-time point ^{18}F-FDG PET

We also determined the relationship between short term disease progression and dual-time point ^{18}F-FDG PET findings in patients with IIP. There was no significant

difference in early SUV level between patients with progressive IIPs and stable ones (Table 5). In contrast, the RI-SUVs were significantly higher in patients with progressive IPF and NSIP (13.0±8.9%) compared to patients with stable IPF and NSIP (-16.8±5.9%, $P < 0.0001$, analyzed by the Steel-Dwass test). The progressive COP group (19.8±6.0%) had a tendency to increase the RI-SUVs compared to patients with stable COP (-16.6±13.3%, $P = 0.056$). Figure 2B shows the distribution of RI-SUV levels for lung lesions in patients with IIPs. ROC curve analysis indicated that the most suitable cut-off value for RI-SUV at lung lesions was 0% to distinguish the progressive from stable IIP group. When using a RI-SUV threshold of 0% to differentiate progressive IIP, sensitivity, specificity, and accuracy were 95.5%, 100%, and 97.8%, respectively. In addition, when the analysis was limited to surgically confirmed cases, the RI-SUVs were significantly higher in patients with progressive IPF and NSIP (13.1±10.3%, n=12) compared to patients with stable IPF and NSIP (-16.4±6.9%, $P = 0.0001$, analyzed by the Steel-Dwass test, n=15). There was no significant difference between progressive COP group (19.2±3.6%, n=3) and stable COP (-20.9%, $P = 0.26$, n=2). In surgically confirmed cases, when using a RI-SUV threshold of 0% to differentiate progressive IIP, sensitivity, specificity, and accuracy were 93.3%, 100%, and 96.9%, respectively.

Representative ^{18}F-FDG PET images used for evaluation of disease progression in pathologically diagnosed fibrotic NSIP cases are shown in Figures 3 and 4. One patient with NSIP who had evidence of deterioration in pulmonary function three months after the ^{18}F-FDG PET scan (progressive NSIP, Figure 3) had a positive RI-SUV value (24.3%), while a patient with NSIP who did not show deterioration of pulmonary function at one year after ^{18}F-FDG PET scanning (stable NSIP, Figure 4) had a negative RI-SUV value (-22.0%).

DISCUSSION

In the present study of 50 patients with IIP, we found that the early SUV (cut-off: 1.5) in COP was significantly higher than that in IPF and NSIP with reasonable sensitivity and specificity, although no significant difference between IPF and NSIP was observed. On the other hand, a positive value of RI-SUV (cut-off: 0%) predicts the deterioration of pulmonary function within a 1-year observation period in patients with IIP. However, early SUV was not a significant predictor of disease progression.

Regarding with image diagnosis of IIPs, the early SUV level of ^{18}F-FDG PET could be useful for distinguishing COP from IPF and NSIP. According to the ATS/ERS consensus classification of IIPs [1], the main histopathologic feature of COP is a patchy process characterized primarily by organizing pneumonia involving variable numbers of inflammatory cells, such as lymphocytes, macrophages, and neutrophils, with a lower degree of interstitial fibrosis, as compared to IPF and NSIP. Nagai et al. noted that increased cell recovery and percentage of lymphocytes in BAL fluid were found in patients with COP, compared to those with IPF [16]. These findings suggest that the degree of inflammatory cell infiltrates has an effect on early SUV in IIP.

Our results also indicate that RI-SUV is useful for determining disease activity as a predictor of disease progression. Although hiatopathological diagnosis is related to

response to treatment as well as survival in IIP patients [16], a recent report showing a high mortality rate (21.7%) for patients with IPF after surgical lung biopsy has raised safety concerns and initiated debate regarding surgical lung biopsy procedures for IPF patients [3]. Furthermore, the natural histories of IPF and NSIP are not well defined. Although the course of IPF is typically described as a relentless decline in respiratory function, individual courses are highly variable and some patients remain stable for extended periods of time without treatment [17]. On the other hand, the survival rates of patients with NSIP vary considerably among studies. Travis et al. reported a 5-year survival rate of 90% for NSIP [18], whereas Nicholson et al. found it to be only 45% [19]. This variability and considerable overlap in patient survival on the basis of these pathologic patterns [16, 18, 19] indicate a need to define other non-invasive prognostic parameters.

Recently, several studies have shown that serial changes in dyspnea and lung function are predictive markers of survival in IIP [20-23]. In particular, deterioration in forced vital capacity and D_{LCO} during the initial 6 to12 months is a stronger predictor of survival than pathological diagnosis in IPF and NSIP patients [22, 23]. However, these serial physiologic parameters cannot be assessed at the time of initial presentation. Since RI-SUV could predict the deterioration of pulmonary function after 12 months of

follow-up examinations, it has potential as a predictor of survival in IPF and NSIP patients at the time of diagnosis.

Tumoral FDG uptake does not reach its maximum value until 5 hours after administration [24], whereas benign inflammatory lesions and physiologic FDG uptake lesions show a stable pattern or a slight decline [25]. However, a recent report showed that the increase in ^{18}F-FDG uptake between early and delayed PET images is a predictor for activity of pulmonary tuberculoma [9]. In addition, activation of inflammatory cells causes a sustained increase in FDG accumulation over time [10-12]. These findings suggest that inflammatory cell activity is associated with sustained FDG uptake (positive RI-SUV value) in progressive IIP lung.

Based on the data presented, it might be possible to use dual-time point ^{18}F-FDG PET imaging to classify IIPs into four groups, and for management of IIPs (Fig. 5), as follows: 1) High early SUV level (> 1.5) and positive RI-SUV (> 0%) correspond to progressive COP patients. Since it is predicted that patients will have deterioration of pulmonary function in the short term and good response to corticosteroid therapy, corticosteroid therapy is required; 2) High early SUV level (> 1.5) and negative RI-SUV (< 0%) could correspond to stable COP patients, and patients could be expected to show improvement within a 1-year observation period; 3) Low early SUV

level (< 1.5) and positive RI-SUV (> 0%) are progressive IPF and NSIP patients. Since it is predicted that patients will have deterioration of pulmonary function within 12 months and poor to moderate response to corticosteroid therapy, other treatment options may be required (e.g. immunosuppressants); and 4) Low early SUV level (< 1.5) and negative RI-SUV (< 0%) are stable IPF and NSIP patients. Since it is predicted that patients will not show deterioration of pulmonary function within 12 months and usually have poor response to corticosteroid treatment, immediate corticosteroid therapy may not be required.

In conclusion, this first and preliminary study indicates that dual-time point ^{18}F-FDG PET can provide non-invasive information for characterization of IIP as well as a prediction of disease progression and responsiveness to treatment with corticosteroids at the time of initial presentation. In the future, it will be necessary to clarify the usefulness of dual-time point ^{18}F-FDG PET imaging using a prognostic marker of IIPs, especially of IPF and NSIP, with a larger series of patients and longer follow-up period.

ACKNOWLEDGMENTS

We thank Dr Norihiro Naiki (Department of Molecular Pathology, University of

Fukui) for valuable advice regarding pathological diagnosis.

This work was supported by the 21st Century COE program “Biomedical Imaging Technology Integration Program” from the Japan Society of the Promotion of Science (JSPS).

REFERENCES

1. American Thoracic Society/European Respiratory Society International Multidisciplinary Consensus Classification of the Idiopathic Interstitial Pneumonias. *Am J Respir Crit Care Med.* 2002;165:277-304.

2. Park JH, Kim DK, Kim DS, et al. Mortality and risk factors for surgical lung biopsy in patients with idiopathic interstitial pneumonia. *Eur J Cardiothorac Surg.* 2007;31:1115-1119.

3. Utz JP, Ryu JH, Douglas WW, et al. High short-term mortality following lung biopsy for usual interstitial pneumonia. *Eur Respir J.* 2001;17:175-179.

4. Monaghan H, Wells AU, Colby TV, du Bois RM, Hansell DM, Nicholson AG. Prognostic implications of histologic patterns in multiple surgical lung biopsies from patients with idiopathic interstitial pneumonias. *Chest.* 2004;125:522-526.

5. Demura Y, Tsuchida T, Ishizaki T, et al. 18F-FDG accumulation with PET for differentiation between benign and malignant lesions in the thorax. *J Nucl Med.* 2003;44:540-548.

6. Shin L, Katz DS, Yung E. Hypermetabolism on F-18 FDG PET of multiple pulmonary nodules resulting from bronchiolitis obliterans organizing pneumonia. *Clin Nucl Med*. 2004;29:654-656.

7. Meissner HH, Soo Hoo GW, Khonsary SA, Mandelkern M, Brown CV, Santiago SM. Idiopathic pulmonary fibrosis: evaluation with positron emission tomography. *Respiration.* 2006;73:197-202.

8. Morikawa M, Demura Y, Mizuno S, Ameshima S, Ishizaki T, Okazawa H. FDG positron emission tomography imaging of drug-induced pneumonitis. *Ann Nucl Med.* 2008;22:335-338.

9. Kim IJ, Lee JS, Kim SJ, et al. Double-phase ^{18}F-FDG PET-CT for determination of pulmonary tuberculoma activity. *Eur J Nucl Med Mol Imaging*. 2008;35:808-814.

10. Deichen JT, Prante O, Gack M, Schmiedehausen K, Kuwert T. Uptake of [18F]fluorodeoxyglucose in human monocyte-macrophages in vitro. *Eur J Nucl Med Mol Imaging.* 2003;30:267-273.

11. Ishimori T, Saga T, Mamede M, et al. Increased (18)F-FDG uptake in a model of inflammation: concanavalin A-mediated lymphocyte activation. *J Nucl Med.* 2002;43:658-663.

12. Schuster DP, Brody SL, Zhou Z, et al. Regulation of lipopolysaccharide-induced increases in neutrophil glucose uptake. *Am J Physiol Lung Cell Mol Physiol.* 2007;292:845-851.

13. Watters LC, King TE, Schwarz MI, Waldron JA, Stanford RE, Cherniack RM. A

clinical, radiographic, and physiologic scoring system for the longitudinal assessment of patients with idiopathic pulmonary fibrosis. *Am Rev Respir Dis* 1986;133:97-103.

14. ATS/ERS Standardization of Lung Function Testing: General Considerations for Lung Function Testing. *Eur Respir J.* 2005;26:153-161.

15. American Thoracic Society. Idiopathic pulmonary fibrosis: diagnosis and treatment. International consensus statement. American Thoracic Society (ATS), and the European Respiratory Society (ERS). *Am J Respir Crit Care Med.* 2000;161:646-664.

16. Nagai S, Kitaichi M, Itoh H, Izumi T, Colby TV. Idiopathic nonspecific interstitial pneumonia/fibrosis: comparison with idiopathic pulmonary fibrosis and BOOP. *Eur. Respir. J.* 1998;12:1010-1019.

17. Kim DS, Collard HR, King TE Jr. Classification and natural history of the idiopathic interstitial pneumonias. *Proc Am Thorac Soc*. 2006;3:285-292.

18. Travis WD, Matsui K, Moss J, Ferrans VJ. Idiopathic nonspecific interstitial pneumonia: prognostic significance of cellular and fibrosing patterns: survival comparison with usual interstitial pneumonia and desquamative interstitial pneumonia. *Am J Surg Pathol.* 2000;24:19-33.

19. Nicholson AG, Colby TV, du Bois RM, Hansell DM, Wells AU. The prognostic significance of the histologic pattern of interstitial pneumonia in patients presenting

with the clinical entity of cryptogenic fibrosing alveolitis. *Am J Respir Crit Care Med.* 2000;162:2213-2217.

20. Collard HR, King TE Jr, Bartelson BB, Vourlekis JS, Schwarz MI, Brown KK. Changes in clinical and physiologic variables predict survival in idiopathic pulmonary fibrosis. *Am J Respir Crit Care Med.* 2003;168:538-542.

21. Flaherty KR, Mumford JA, Murray S, et al. Prognostic implications of physiologic and radiographic changes in idiopathic interstitial pneumonia. *Am J Respir Crit Care Med.* 2003;168:543-548.

22. Jegal Y, Kim DS, Shim TS, et al. Physiology is a stronger predictor of survival than pathology in fibrotic interstitial pneumonia. *Am J Respir Crit Care Med.* 2005;171:639-644.

23, Latsi PI, du Bois RM, Nicholson AG, et al. Fibrotic idiopathic interstitial pneumonia: the prognostic value of longitudinal functional trends. *Am J Respir Crit Care Med.* 2003;168:531-537.

24. Hamberg LM, Hunter GJ, Alpert NM, Choi NC, Babich JW, Fischman AJ. The dose uptake ratio as an index of glucose metabolism: useful parameter or oversimplification? *J Nucl Med*. 1994;35:1308-1312.

25. Hustinx R, Smith RJ, Benard F, et al. Dual time point fluorine-18 fluorodeoxyglucose positron emission tomography: a potential method to differentiate malignancy from inflammation and normal tissue in the head and neck. *Eur J Nucl Med*. 1999;26:1345-1348.

Table 1 Patient characteristics

	Number of cases
(1) Patients	50
Sex (M/F)	21/29
Mean age (years, mean±SD)	66.2±11.6
Age range (years)	21-84

(2) Diagnosis	Number of cases	Progressive IIP	Stable IIP
IPF	21	8	13
NSIP	18	9	9
COP	11	8	3
Total	50	25	25

Abbreviations: IIP = idiopathic interstitial pneumonia; IPF = idiopathic pulmonary fibrosis; NSIP = nonspecific interstitial pneumonia; COP = cryptogenic organizing pneumonia.

Table 2 Clinical feature, serum markers, selected pulmonary function indices, and radiologic features of study participants

	IPF (n=21)	NSIP (n=18)	COP (n=11)
Dyspnea score (0-20)	8.1±2.7	7.6±2.5	8.0±3.3
KL-6 (U/mL)	828±652 †	1363±917 †	329±98
SP-D (ng/mL)	156±108	253±234	165±132
Resting PaO_2 (mmHg)	82.9±10.5*	76.7±8.1 †	67.3±9.1
VC, % predicted	83.2±27.0	79.9±21.4	77.6±18.8
D_{LCO}, % predicted	56.4±21.2	53.7±16.5	60.2±23.9
HRCT findings (n)			
Honeycomb	19/21	3/18	
Consolidation	7/21	10/18	10/11
GGO and reticular density	21/21	18/18	10/11

Values express the mean±SD.

The Kruskal-Wallis test analyzed multiple group comparisons and Steel-Dwass test assessed between-group comparisons.

* $P < 0.01$, versus COP.

† $P < 0.05$, versus COP.

Table 3 Comparison of early SUV in IIP according to chest CT findings on an individual patient basis

CT findings	IPF	NSIP	COP
Abnormal shadow	0.99±0.29 †] *	1.22±0.44 †] *	2.47±0.74] *
Normal	0.57±0.12	0.67±0.18	0.70±0.25

Values express the mean±SD.

The Kruskal-Wallis test analyzed overall group comparisons and Steel-Dwass test assessed between-group comparisons.

* $P < 0.01$.

† $P < 0.01$, versus COP.

Abbreviations: IIP = idiopathic interstitial pneumonia; CT = computed tomography; IPF = idiopathic pulmonary fibrosis; NSIP = nonspecific interstitial pneumonia; COP = cryptogenic organizing pneumonia.

Table 4 Comparison of early SUV in each lesion type according to chest HRCT findings

HRCT findings	IPF	NSIP	COP
Honeycomb	1.32±0.47* ┐	1.90±0.48 † ┐	
Consolidation	1.39±0.51 † ┘ **ns**	1.72±0.62* ┘ **ns**	3.67±1.25*
GGO and reticular density	0.82±0.23	1.15±0.38	1.87±0.56

Values express the mean±SD.

The Kruskal-Wallis test analyzed multiple group comparisons and statistical significance of difference among three groups of HRCT finding was calculated using Steel-Dwass test.

* $P < 0.01$, versus GGO.

† $P < 0.05$, versus GGO.

Table 5 Comparison of early SUV and RI-SUV between NSIP, IPF group and COP

	NSIP and IPF		COP	
	Progressive (n=17)	**Stable (n=22)**	**Progressive (n=8)**	**Stable (n=3)**
Early SUV	1.21±0.50*	1.01±0.20 †	2.51±0.76	2.36±0.51
RI-SUV (%)	13.0±8.9‡	-16.8±5.9	19.8±6.0§	-16.6±13.3

Values express the mean±SD.

The Kruskal-Wallis test analyzed multiple group comparisons and Steel-Dwass test assessed between-group comparisons.

* $P < 0.01$, versus progressive COP.

† $P < 0.05$, versus stable COP.

‡ $P < 0.0001$, versus stable NSIP and IPF.

§ $P = 0.056$, versus stable COP.

Figure Legends

Fig. 1 Six circular ROIs (30 mm in diameter) drawn on bilateral lungs at three representative slice levels with reference to individual CT images

ROIs for normal lung (broken line) and consolidation (solid line) were defined by corresponding CT images.

Fig. 2 Box plot of early SUV (A) and retention index (RI-SUV) (B) in patients with IPF (progressive, n = 8; stable, n = 13), NSIP (progressive, n = 9; stable, n = 9), and COP (progressive, n = 8; stable, n = 3)

(A) Receiver operating characteristic (ROC) curve analysis determined that the most suitable cut-off value for early SUV at lung lesions was 1.5 (broken line) to distinguish COP from the IPF and NSIP groups. (B) ROC curve analysis indicated that the most suitable cut-off value for RI-SUV at lung lesions was 0% (broken line) to distinguish the progressive from stable IIP group. Box plots show the 10th, 25th, 75th, and 90th percentiles, as well as the median.

Fig. 3 A 70-year-old woman with pathologically diagnosed NSIP

Deterioration of pulmonary function was seen at 3 months after ^{18}F-FDG PET scanning

and she died 3 years after the initial diagnosis because of respiratory dysfunction. (A) Chest HRCT showing ground-glass opacities and reticular shadows in both lung fields. (B) Transaxial ^{18}F-FDG PET (early imaging) showing ^{18}F-FDG accumulation in lesions with abnormal shadows on corresponding CT images. (C) ^{18}F-FDG PET (delayed imaging) showing increased ^{18}F-FDG accumulation compared to early imaging (RI-SUV = 24.3%).

Fig. 4 A 73-year-old woman with pathologically diagnosed NSIP

No deterioration of pulmonary function was seen 1 year after ^{18}F-FDG PET scanning. (A) Chest HRCT showing ground-glass opacities and reticular shadows in both lung fields. (B) Transaxial ^{18}F-FDG PET (early imaging) showing ^{18}F-FDG accumulation in lesions with abnormal shadows on corresponding CT images. (C) ^{18}F-FDG PET (delayed imaging) showing decreased ^{18}F-FDG accumulation compared to early imaging (RI-SUV = -22.0%).

Fig. 5 Schematic drawing of proposed diagnosis of disease type and activity with dual-time point ^{18}F-FDG PET

It might be possible to use dual-time point ^{18}F-FDG PET to classify IIPs into four

groups. The early SUV (cut-off level: 1.5) can distinguish COP from IPF and NSIP. On the other hand, the RI-SUV (cut-off level: 0%) can predict short term (1 year) disease progression, with a positive RI-SUV value predicting deterioration of pulmonary function within a 1-year observation period and a negative RI-SUV value predicting a spontaneous remission or no evidence of deterioration of pulmonary function within a 1-year observation period.

Figure1

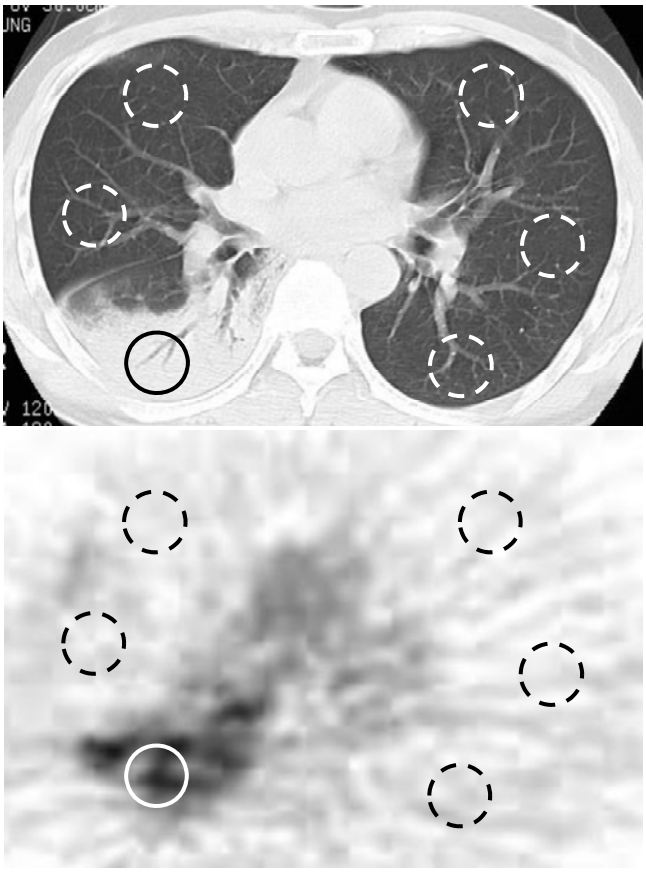

Figure2

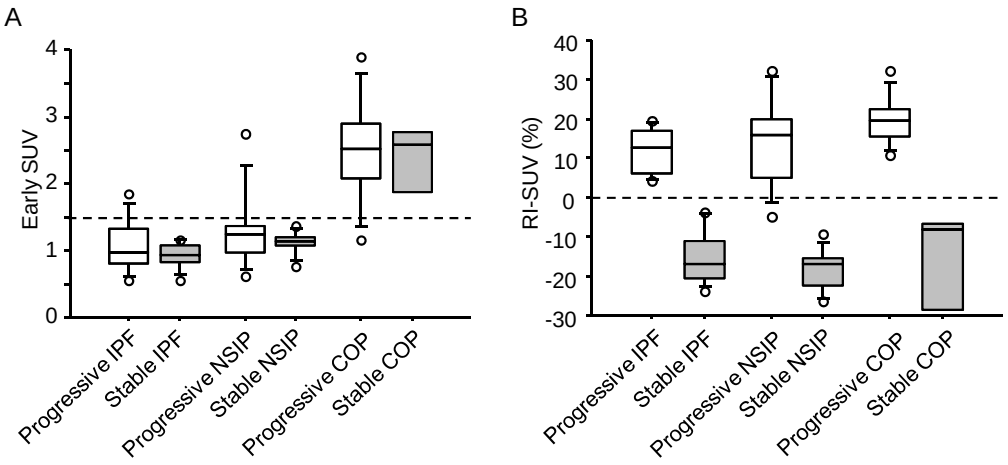
A
Early SUV
4
3
2
1
0
Progressive IPF
Stable IPF
Progressive NSIP
Stable NSIP
Progressive COP
Stable COP
B
RI-SUV (%)
40
30
20
10
0
-10
-20
-30
Progressive IPF
Stable IPF
Progressive NSIP
Stable NSIP
Progressive COP
Stable COP

Figure3

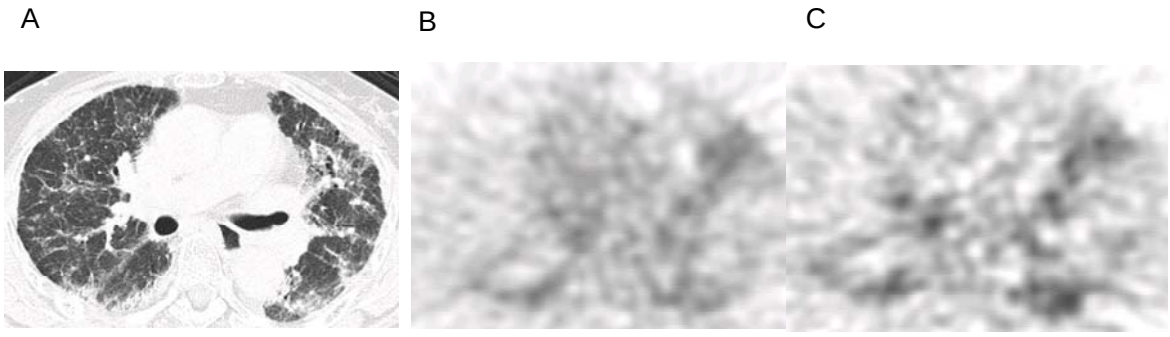

Figure4

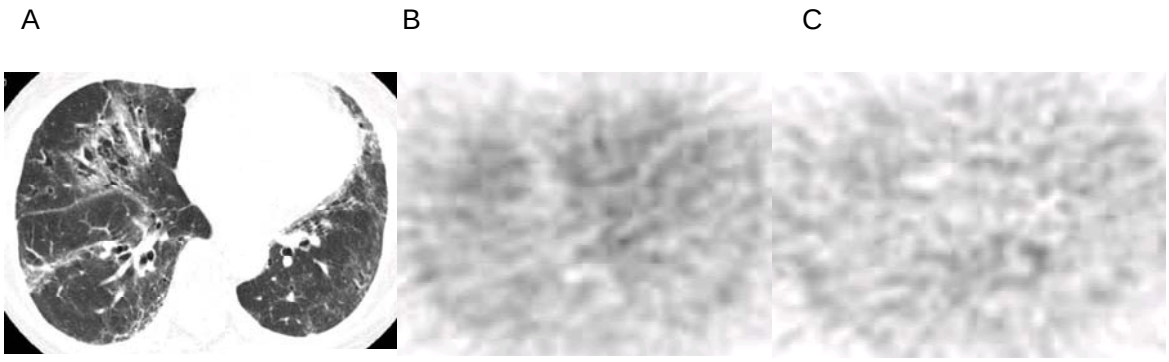

Figure5

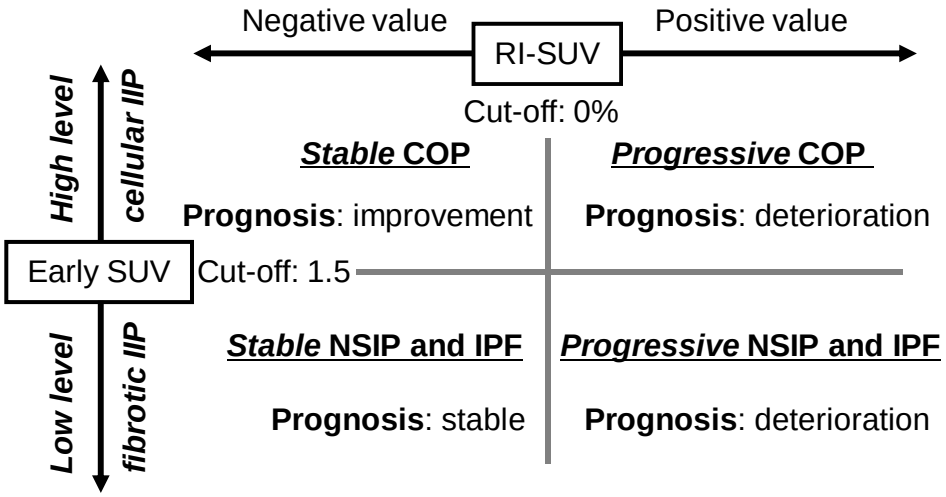
Negative value
RI-SUV
Positive value
Cut-off: 0%
High level
cellular IIP
Stable COP
Progressive COP
Prognosis: improvement
Prognosis: deterioration
Early SUV
Cut-off: 1.5
Low level
fibrotic IIP
Stable NSIP and IPF
Progressive NSIP and IPF
Prognosis: stable
Prognosis: deterioration